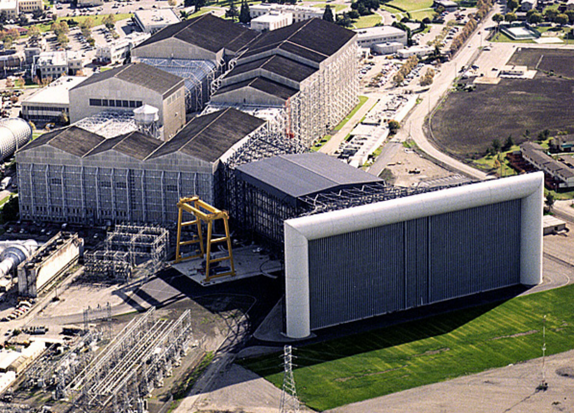


NASA

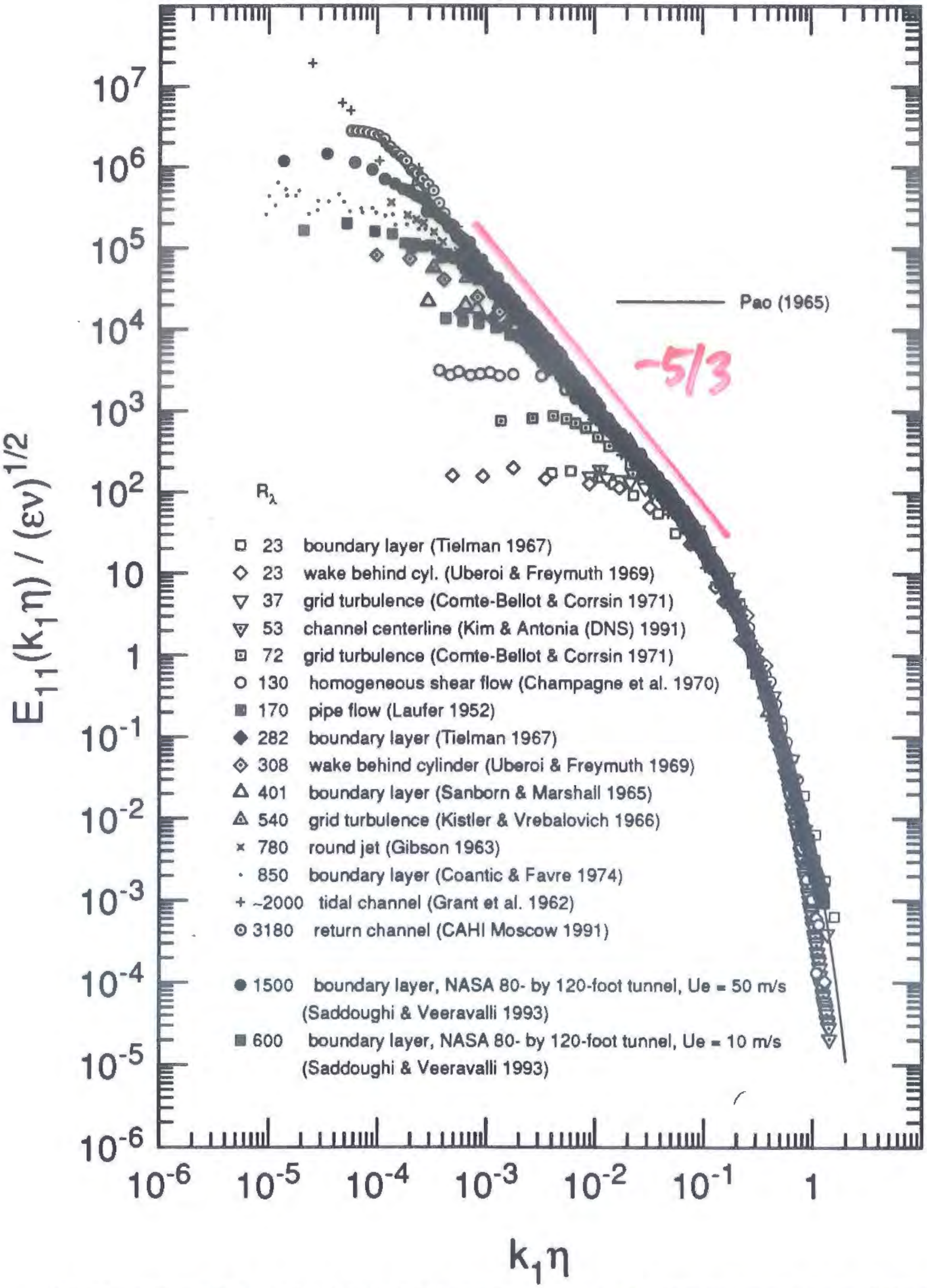

Kolmogorov scaling for the longitudinal spectra measured in the boundary layer of the 80- by 120-foot wind tunnel at NASA Ames compared with data from other experiments. This compilation is from Chapman (1979) with later additions.

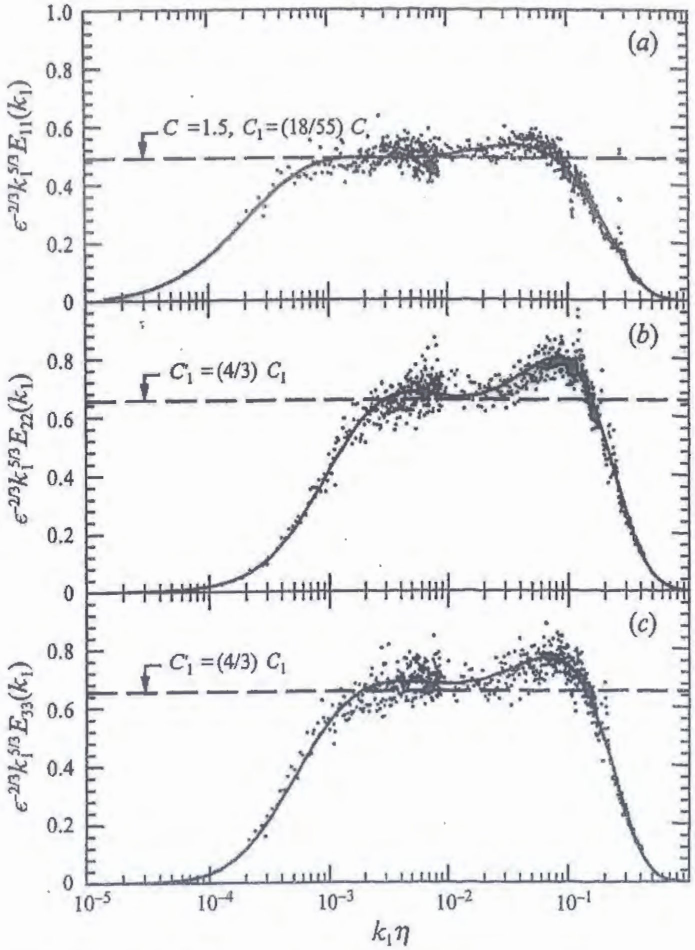

FIGURE 13. Compensated longitudinal and transverse spectra measured at mid-layer for the high-speed case ($y = 400$ mm, $y^+ \approx 62000$, $R_\lambda \approx 1450$). Only the data for wavenumber range $k_1 \eta < 0.25$ can be accepted. Solid lines are the ninth-order, least-square, log-log polynomial fits to the spectral data. (a) u_1-spectrum; (b) u_2-spectrum; (c) u_3-spectrum.

3.2.2. *Inertial subrange*

To investigate the validity of (7) and (8) in the inertial subrange, we again analyse the compensated spectra $\epsilon^{-\frac{2}{3}} k_1^{\frac{5}{3}} E_{\alpha\alpha}(k_1)$. In the inertial subrange, these should be independent of wavenumber and equal to the Kolmogorov's constants for one-dimensional spectra.

In figure 12 the compensated longitudinal and transverse spectra at the mid-layer position in the low-speed case, are plotted against $k_1 \eta$. The compensated ninth-order, least-square polynomial log-log fits of $E_{\alpha\alpha}(k_1)$ presented in this figure prove to be very instructive in analysing the data. Here the dissipation value ($\epsilon \approx 0.33\ \mathrm{m^2\ s^{-3}}$) obtained in the previous section is used.

For the u_1-spectrum there is slightly less than one decade of $-\frac{5}{3}$ range, and in that wavenumber range the classical value for the Kolmogorov constant, $C = 1.5$ (i.e. $C_1 = 18C/55 = 0.491$) (Monin & Yaglom 1975) agrees very well with the present data. Noting that our dissipation accuracy was $\pm 10\%$, this gives $C = 1.5 \pm 0.1$. The u_3-spectrum exhibits more than half a decade of $-\frac{5}{3}$ range, with an amplitude equal to $\frac{4}{3}$

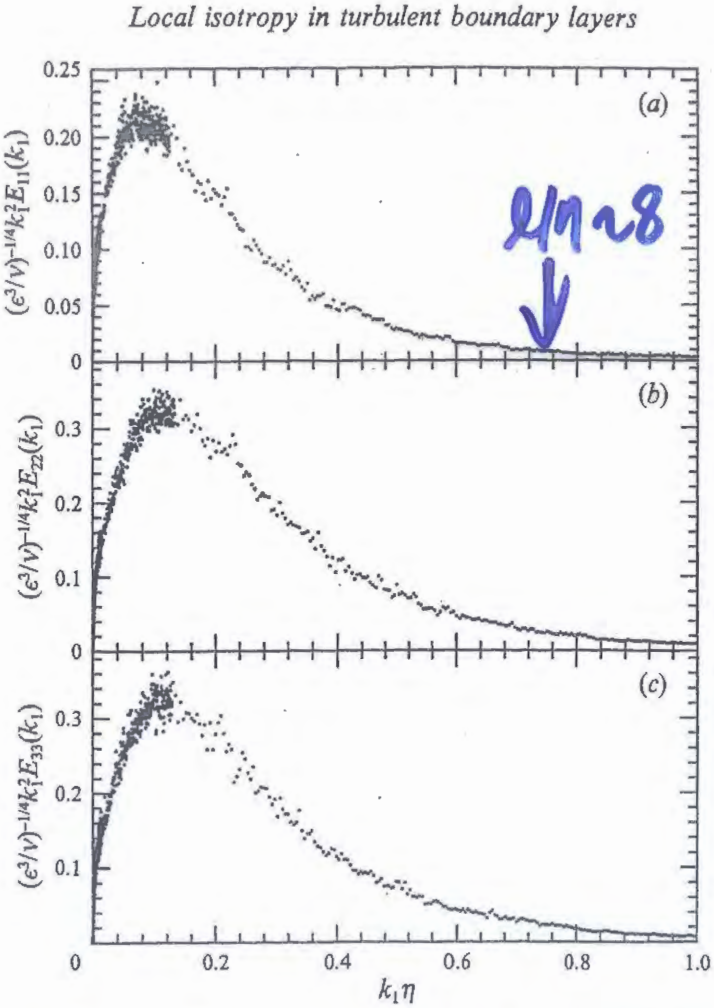

FIGURE 10. Dissipation spectra measured at mid-layer for the low-speed case ($y = 515$ mm, $R_\lambda \approx 600$). (*a*) u_1-spectrum; (*b*) u_2-spectrum; (*c*) u_3-spectrum.

3.2.1. *Dissipation range*

At the mid-layer position of the low-speed case ($y = 515$ mm, $R_\lambda \approx 600$), dissipation spectra given by the isotropic relation (Batchelor 1953)

$$\epsilon = 15\nu \int_0^\infty k_1^2 E_{11}(k_1)\,\mathrm{d}k_1 = \tfrac{15}{2}\nu \int_0^\infty k_1^2 E_{22}(k_1)\,\mathrm{d}k_1 = \tfrac{15}{2}\nu \int_0^\infty k_1^2 E_{33}(k_1)\,\mathrm{d}k_1, \qquad (24)$$

are plotted in non-dimensional form in figure 10. From the areas (before normalization) under the curves (*a*), (*b*) and (*c*) the values of $\overline{(\partial u_1/\partial x_1)^2}$, $\overline{(\partial u_2/\partial x_1)^2}$, and $\overline{(\partial u_3/\partial x_1)^2}$, respectively, can be calculated. It is clear that for this case the entire significant range of the dissipation spectrum is obtained. The scatter of the data around the peak is the result of superimposing the three measurement segments. This scatter is about $\pm 10\%$ and, as will be shown later, the data for $k_1\eta > 0.8$ may not be reliable. The integration over the third-spectral band of this data, which covered the entire frequency range of interest, satisfied (24) to within 10%; the dissipation value obtained from the single-wire data shown in figure 10(*a*) is $\epsilon \approx 0.33\ \mathrm{m^2\,s^{-3}}$. Similar integrations were performed for the inner-layer position of the low-speed case and satisfied (24) to within 15%. There the dissipation value is $\epsilon \approx 3.1\ \mathrm{m^2\,s^{-3}}$.